JOURNAL OF GEOPHYSICAL RESEARCH: SPACE PHYSICS, VOL. 118, 912–918, doi:10.1002/jgra.50109, 2013

Production of very high potential differences by intracloud lightning discharges in connection with terrestrial gamma ray flashes

Sotirios A. Mallios,[1] Sebastien Celestin,[1,2] and Victor P. Pasko[1]

Received 3 October 2012; revised 11 December 2012; accepted 4 January 2013; published 28 February 2013.

[1] Terrestrial gamma-ray flashes (TGFs) have been correlated with an early development stage of high altitude positive intracloud (+IC) flashes in which the negative leader propagates up toward the upper positive charge region, while the positive leader propagates down toward the lower negative charge region. The resultant bidirectional leaders develop electrical potential differences in the vicinity of their heads with respect to the ambient potential distribution created by the thundercloud charges. These potential differences are believed to be of essential importance for the generation of TGFs. Using electrostatic calculations and a three-dimensional Cartesian fractal model, we quantify these potential differences produced in a developing +IC lightning discharge for given thunderstorm electric configurations. We present a case of a +IC lightning discharge in a realistic thunderstorm configuration that leads to a very high (~300 MV) potential difference and show how a delay in the development of the negative leader with respect to the positive one in a bidirectional leader system can facilitate a high potential difference in the negative leader head region.

Citation: Mallios, S. A., S. Celestin, and V. P. Pasko (2013), Production of very high potential differences by intracloud lightning discharges in connection with terrestrial gamma ray flashes, *J. Geophys. Res. Space Physics*, *118*, 912–918, doi:10.1002/jgra.50109.

1. Introduction

[2] A leader discharge can be defined as a thin, highly ionized, and highly conducting channel that grows from the strong field region along the path prepared by preceding streamers [*Raizer*, 1991, p. 364]. The leader process is known to be a valid propagation mechanism for intracloud (IC) lightning discharges [*Ogawa and Brook*, 1964; *Proctor*, 1981; *Uman*, 1984, p. 10; *Liu and Krehbiel*, 1985; *Shao and Krehbiel*, 1996; *Rakov and Uman*, 2003, p. 322]. Bidirectional leaders that initiate IC discharges develop electric potential differences in their heads with respect to the ambient potential on the order of tens of MV as they extend over distances of several kilometers [e.g., *Celestin and Pasko*, 2011, and references therein].

[3] High altitude +IC flashes (the negative leader propagates up toward the upper positive charge region, whereas the positive leader propagates down toward the lower negative charge region) have been correlated with terrestrial gamma-ray flashes (TGFs) [*Williams et al*., 2006; *Stanley et al*., 2006]. TGFs are high energy photon bursts originating from the Earth's atmosphere caused by the brehmsstrahlung emission from energetic electrons. These bursts are observed by space-born detectors in low Earth orbit [*Fishman et al*., 1994; *Smith et al*., 2005; *Marisaldi et al*., 2010; *Briggs et al*., 2010]. *Shao et al*. [2010] and *Lu et al*. [2010, 2011] observed that TGFs occurred within the initial milliseconds of +IC flashes, while the negative leader had developed upward. During this stage, the advancement of the negative lightning leader is believed to be made by the stepping processes [*Shao et al*., 2010; *Lu et al*., 2010].

[4] *Celestin and Pasko* [2011] suggested that the high electric potential difference between the leader head of long unbranched +IC lightning leaders and the ambient potential can be harvested by electrons and can lead to the production of sufficient number of thermal runaway electrons to explain TGFs without invoking further amplification in relativistic runaway electron avalanches (RREAs) in the large-scale ambient electric field of the thunderstorm [e.g., *Gurevich et al*., 1992; *Dwyer*, 2008].

[5] In this paper, using a 3-D Cartesian fractal model, we quantify the electric potential produced in a developing +IC lightning discharge for given thunderstorm electric configurations. This allows for determining the electric potential difference between the lightning leader and the large-scale thunderstorm potential in the region of the leader head. We present a case of a +IC lightning discharge in a realistic thunderstorm configuration that leads to very high potential difference between the

[1]Communications and Space Sciences Laboratory, Department of Electrical Engineering, Penn State University, University Park, Pennsylvania, USA.

[2]Now at Laboratory of Physics and Chemistry of the Environment and Space (LPC2E), Observatory of Sciences of the Universe in the French Center region (OSUC), University of Orleans, CNRS, Orleans Cedex 2, France.

Corresponding author: Sotirios A. Mallios, Communications and Space Sciences Laboratory, Department of Electrical Engineering, Penn State University, University Park, Pennsylvania, USA. (sxm5245@psu.edu)

2169-9380/13/10.1002/jgra.50109

leader head and the ambient potential (~300 MV). We demonstrate that specific thundercloud configuration can create very high potential cases, and we show how a delay in the development of the negative leader with respect to the positive one in a bidirectional leader system can produce a high potential difference in the negative leader head region. The impact of these results on the production of TGFs is discussed.

2. Model Formulation

[6] In this work, we model the IC lightning discharge using a 3-D Cartesian fractal model similar to that developed by *Riousset et al.* [2007]. The ground ($z = 0$ km) is assumed to be a perfect electric conductor (maintained at potential $\phi = 0$ V), while the potential over the upper and side boundaries is the result of the contribution of all the charges in the simulation domain as well as their ground images [*Riousset et al.*, 2007]. Assuming a dipolar charge structure for the thundercloud (main upper positive and lower negative charge layers), we set the two charge layers to be cylindrical disks (Figure 1c). The main negative charge region is typically found in a temperature range roughly -10 to -25°C [*Rakov and Uman*, 2003, p. 75], which corresponds to an altitude range 4–6 km. We choose the center of the main negative charge to be at altitude $h_- = 6$ km, while the altitude of the positive charge is chosen to be at $h_+ = 11$ km, which is in the range of 10–14 km where the main positive charge region is typically found [*Rakov and Uman*, 2003, p. 76]. The horizontal dimensions of active air-mass thunderstorms range from about 3 to >50 km [*Rakov and Uman*, 2003, p. 68]. We choose the radii of the charge regions to be $R_\pm = 15$ km, that are in this range. We note that for this configuration a factor of 3 difference between the charge regions' radii and the vertical distance between the charge regions creates an electric field that is approximately uniform in the region between them. The vertical widths of the charge regions are chosen to be $W_\pm = 1.5$ km. The development of the discharge tree starts at a point where the ambient electric field exceeds a predefined initiation threshold for a lightning discharge by 10%. This threshold is chosen to be $E_{\text{init}} = 2.16$ kV/cm at sea level, which is similar to that used in studies by *Krehbiel et al.* [2004] and *Marshall et al.* [2005]. For the chosen charge geometry, the amount of charge that is needed for the ambient electric field to exceed the E_{init} by 10% is $Q_\pm = \pm 577.35$ C.

[7] We calculate the potential in the simulation domain by solving Poisson's equation $\nabla^2\phi = -\rho/\varepsilon_0$, where ρ is the volumetric charge distribution of the charge layers and ε_0 is the permittivity of free space, using a successive over

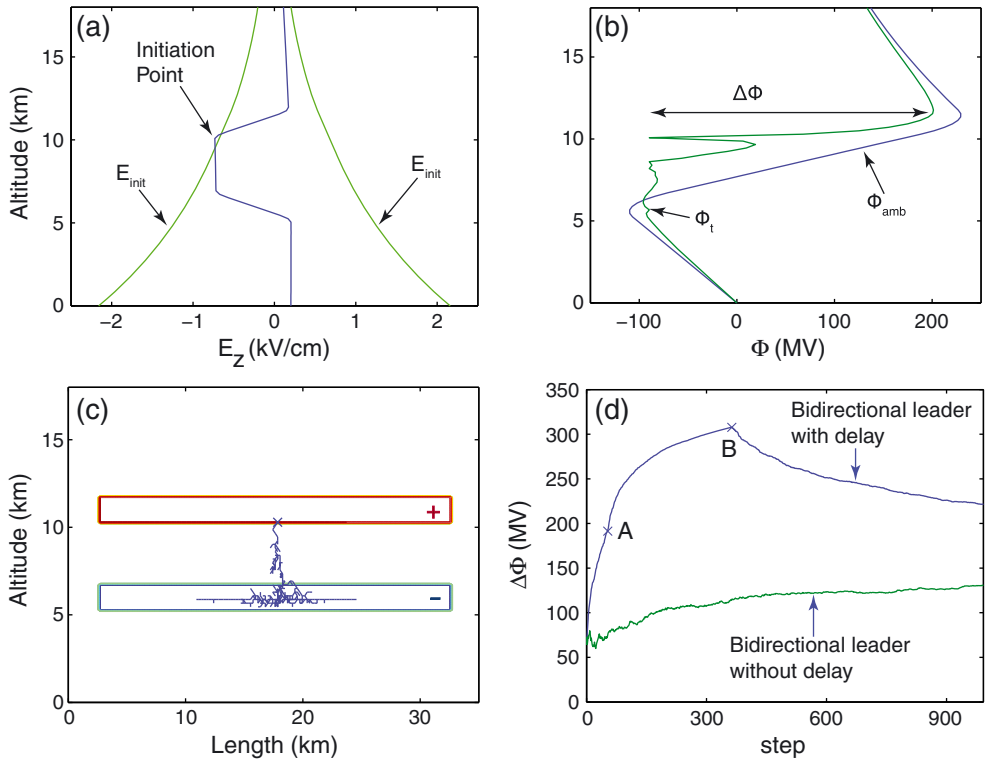

Figure 1. Case of a +IC lightning. (a) Ambient electric field distribution along the axis of the simulation domain. (b) Potential distribution along the axis of the simulation domain before the lightning development (ϕ_{amb}) and at the simulation step when the potential difference between the negative leader tip and the ambient potential ($\Delta\phi$) is maximum (ϕ_t) in the case of a delay in the negative leader propagation. (c) Cross section of the lightning discharge structure at the step when the potential difference between the negative leader tip and the ambient potential ($\Delta\phi$) is maximum in the case of a delay of the negative leader propagation. (d) Potential difference between the negative leader tip and the ambient potential ($\Delta\phi$) at every simulation step. Point A denotes the start of the horizontal development of the positive leader, while point B denotes the initiation point of the negative leader.

relaxation (SOR) algorithm [*Press et al*., 1992, p. 866]. This potential distribution of the cloud charges (referred to as ambient potential ϕ_{amb}) is kept unchanged during the development of the discharge tree, therefore assuming that lightning develops instantaneously when compared to the long time scale thundercloud charge evolution.

[8] The leader channel propagation is modeled iteratively from this location, where the ambient field exceeds the initiation threshold, by adding one new link at every step and updating the potential to ensure the overall charge neutrality of the channel [*Riousset et al*., 2007]. At every step, a new link is randomly chosen among candidates, which are defined as the possible links between the channel points and the neighboring points where the local field exceeds the propagation threshold field of positive or negative leader $E_{th}^{\pm}$ [*Riousset et al*., 2007]. The propagation threshold field is the minimum electric field required for the propagation of the positive and negative leaders. The value of the leader propagation threshold for large laboratory gaps (several tens of meters long) is about 1 kV/cm at sea level [*Raizer*, 1991, p. 363]. After the new link has been selected, a constant potential ϕ_0, which characterizes the equipotential leader channel, is calculated by an iterative method, as the potential which nullifies the total net charge on the channel (see the study by *Riousset et al*. [2007] for a detailed description of the procedures used for the development of the discharge tree). Having calculated the potential in the leader channel, the charge distribution over the channel is calculated and the open boundaries of the simulation domain are updated to include the contribution of the lightning. Finally, the total potential in the simulation domain is obtained by adding the potential created by the charges on the channel to the ambient potential. The whole procedure is repeated until no candidate link for further expansion of the channel is found or until the channel reaches a simulation domain boundary. At every simulation step, the difference between the maximum positive value of the modified ambient potential at the negative leader tip (because of the development of the lightning discharge) and the potential in the leader channel ($\Delta\phi$) is calculated and recorded.

3. Results

[9] In Figure 1, we present the results of the +IC lightning case calculated by our fractal model. In our simulation, to maximize the potential difference between the leader head and the ambient potential (see Discussion section), we allow the negative leader to start propagating only after the positive part of the lightning discharge is fully built. To do this, the propagation threshold of the negative leader is at first set to an artificially large value (~10 times larger than the propagation threshold of the positive leader), while the propagation of the positive leader is set to E_{th}^{+}=1 kV/cm at sea level [*Raizer*, 1991, p. 363]. When the positive part of the lightning discharge cannot develop anymore, we set the propagation threshold of the negative leader to a physical value of E_{th}^{-}=-1 kV/cm at sea level. In Figure 1a, the electric field distribution along the central axis of the domain is shown as a function of the altitude z, just before the development of the +IC lightning discharge. In Figure 1b, the ambient initial potential distribution and the potential distribution after the propagation of the lightning discharge are shown along the central axis of the simulation domain as a function of the altitude at the moment of the maximum potential difference $\Delta\phi$. In Figure 1c, a projection of the lightning discharge structure on the z-y plane at the moment of the maximum potential difference $\Delta\phi$ is shown. The potential difference $\Delta\phi$ is shown in Figure 1d for every step in the simulation.

[10] In Figure 2, the dynamics of the total potential distribution in the presence of the lightning discharge is shown for the case of the IC lightning with a delay in the initiation of the negative leader with respect to the initiation of the positive leader (as in Figure 1) at the steps marked in Figure 1d and at the end of the simulation.

4. Discussion

4.1. Charge Configurations Leading to High Potential Differences in Thunderclouds.

[11] If a perfectly conducting wire is placed in a region with a potential distribution, the wire will acquire potential which lies between the minimum (Φ_{min}) and the maximum (Φ_{max}) value of the ambient potential distribution in the region occupied by the wire. For the case of a straight wire that is placed in a region with linear potential distribution (constant electric field) because of the symmetry of the system and the global neutrality of the isolated conducting wire, the potential drops in the vicinity of the tips of the wire will be equal to $(\Phi_{max} - \Phi_{min})/2$. If the wire expands to regions with higher potential, then the potential in the wire $(\Phi_{max} + \Phi_{min})/2$ will be shifted to higher values. On the other hand, if the wire expands to regions with lower potential, then the potential in the wire will be shifted to lower values.

[12] The above concept is very valuable for defining the conditions under which very high potential difference between the leader head and the ambient potential can occur. The potential in a network of wires depends on the ambient potential distribution. The potential distribution between two

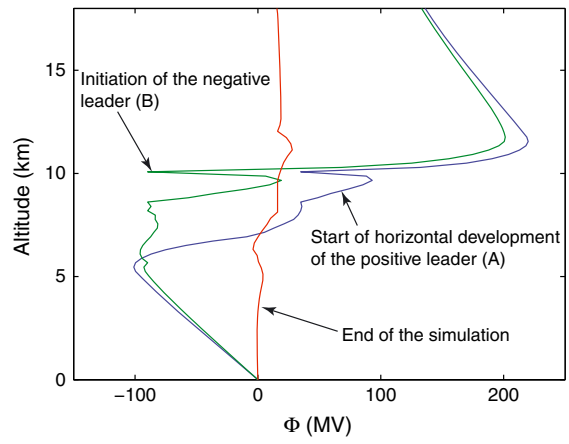

Figure 2. Dynamics of the total potential distribution in the presence of the lightning discharge along the central axis of the simulation domain, in the case of the IC lightning with a delay in the initiation of the negative leader with respect to the initiation of the positive leader at the steps marked in Figure 1d and at the end of the simulation.

charge layers above the conducting ground depends on the total charge in the layers, the distance between these layers, the distance of the lower layer from the ground, and their respective radii. *Celestin and Pasko* [2011] quantitatively demonstrated that if TGFs are directly produced by +IC lightning discharges, the potential difference between the leader channel and the ambient potential would have to be very high. *Xu et al*. [2012] showed that potential differences higher than 100 MV would be necessary to explain the average energy spectrum of TGFs observed by the RHESSI satellite. It is therefore of great interest to explore the thundercloud configurations that would lead to the highest electric potential variation ($\Delta\phi_{\mathrm{amb,max}}$).

[13] One can make a first-order analytical estimate on the conditions that would maximize the potential difference in the cloud as follows. First, to simplify the discussion, let us neglect the influence of the screening charges at the cloud boundaries and the influence of the image charges in the ground. Second, we assume that the electric field is constant between the charge layers (i.e., the charge layer radius is sufficiently large compared to the distance between the charge layers) and is equal to the initiation threshold field at one point only. Therefore, due to the scaling of the lightning initiation field proportionally to the air density, the lightning discharge would always start from nearby the upper charge region. This assumption is fulfilled in our simulations because the radii of the charge layers are three times larger than the distance between them, and as it is clear from Figures 1a and 1c, the initiation point of the lightning discharge is in the vicinity of the upper positive charge region. The initiation threshold for a lightning discharge E_{init} is decreasing exponentially as a function of altitude, and thus, the initiation threshold at a point located at altitude h_{init} can be written as

$$E_{\mathrm{init}}(h_{\mathrm{init}}) = E_{\mathrm{init}}(z=0)e^{-\frac{h_{\mathrm{init}}}{h_s}} \tag{1}$$

[14] where h_s is the atmospheric scale height in the troposphere. Since the electric field between the charge layers is assumed constant, the electrical potential difference between the charge regions can be written as

$$\begin{aligned}\Delta\Phi &= \int_{h_-}^{h_+} E(z)dz = E_{\mathrm{init}}(z=0)e^{-\frac{h_{\mathrm{init}}}{h_s}}(h_+ - h_-) \\ &\simeq E_{\mathrm{init}}(z=0)e^{-\frac{h_+}{h_s}}(h_+ - h_-)\end{aligned} \tag{2}$$

[15] In equation (2), we substituted the h_{init} with h_+ because we assumed that the h_{init} is in the close vicinity of h_+. To find the altitude h_+ that maximizes the potential difference for a given h_-, we differentiate this expression with respect to h_+, and we set the result equal to zero. We find that for a given h_-, the total ambient potential difference is maximized for

$$h_+ - h_- = h_s \tag{3}$$

[16] In the altitude range we are using here ($\leq$15 km), the atmospheric scale height provided by MSISE90 [*Hedin*, 1991] is $h_s \simeq 8.7$ km. Hence, large distances between thundercloud charges would favor high total ambient potential differences, which in turn would favor the occurrence of TGFs. Since a distance between charge layers approaching $h_s \simeq 8.7$ km would imply tall thunderclouds, the maximization of the total ambient potential in a thundercloud might explain why TGFs correspond to high tropopause heights [*Smith et al*., 2010] in addition to the effect of penetration of photons through the atmosphere [*Williams et al*., 2006]. It is also interesting to note that in a limit of small $h_- \ll h_+$, equation (2) gives a maximum possible potential difference in a cloud of $E_{\mathrm{init}}(z=0)h_s/e \simeq 691$ MV (for $E_{\mathrm{init}}(z=0)=2.16$ kV/cm and $h_s=8.7$ km).

[17] Moreover, using RHESSI data, *Splitt et al*. [2010] have concluded that, unlike sprites, there was no strong correlation between the extent of the thundercloud and the occurrence of TGFs. Table 1 illustrates high values of $\Delta\phi_{\mathrm{amb,max}}$ for different thundercloud charges configurations. We note that for every configuration presented in Table 1, the amount of charge in column 1 is the amount that creates electric field which exceeds the initiation threshold for a lightning discharge (2.16 kV/cm at sea level) by 10%. It is interesting to look at the first four rows in Table 1 with regard to this observational result. Indeed, in these four rows, all other parameters being equal (except the charge that is adapted to keep the field consistently 10% above the threshold), only the radius is changed. When the radius becomes greater than the distances between the charge layers, the total variation of the electric potential in the cloud converges to a high value ($\sim$350 MV) that is independent of the radius of the charge layers, effectively reflecting convergence to one-dimensional geometry of the electric field.

[18] The chosen altitudes, distances, and radii of the charge distribution for the case of the +IC lightning discharge presented in Figure 1 correspond to a potential difference equal to 343 MV between the positive and the negative charge layers. Indeed, to explain the production of the highest energy TGFs detected to date [*Tavani et al*., 2011], *Celestin et al*. [2012] assumed that the TGF-producing lightning leader had a potential difference $\Delta\phi$=350 MV with the ambient potential.

[19] In Figure 1a, the z-component of the ambient electric field as a function of altitude is shown, and it is clear that this configuration of charges produces an electric field that is overall lower than the lightning initiation threshold except for a limited region from which the +IC lightning can be initiated.

Table 1. Maximum ambient potential difference (column 5) of two cylindrical charge layers for different values of their total charge (column 1), their altitudes (columns 2 and 3), and their radii (column 4)

$Q_{\pm}$ (C)	h_- (km)	h_+ (km)	$R_{\pm}$ (km)	$\Delta\phi_{\mathrm{amb,max}}$ (MV)
577.35	6	11	15	343
278.17	6	11	10	334.1
86.73	6	11	5	312.6
40.07	6	11	3	284.2
37.08	6	12	3	279.6
41.45	6	10	3	268.4
40.86	6	9	3	228.8
38.57	6	8	3	167.65
46	5	8	3	256.3
36.35	7	10	3	204.17
27.61	9	12	3	155.6

4.2. Experimental Evidence of the Delay in Initiation of the Negative Leader

[20] As we mentioned above, the initiation of an IC lightning discharge is believed to be characterized by the development of a bidirectional lightning leader. The electric field thresholds for initiation and propagation of positive and negative leaders are only documented for laboratory experiments and are known to depend strongly on ambient conditions [*Gallimberti et al*., 2002]. Therefore, the actual electric field thresholds are only approximately known, and their exact values would depend on specific ambient conditions. Moreover, in lightning triggered by rockets carrying an ungrounded wire and in lightning triggered by airplanes, the positive leader is sometimes reported to start 3–6 ms earlier than the negative leader [*Mazur*, 1989; *Laroche et al*., 1991; *Lalande et al*., 1998; *Rakov and Uman*, 2003, p. 354]. Furthermore, due to the fact that the positive leaders radiate weakly in the VHF range and might be missed by the Lightning Mapping Arrays, the precedence of one or the other polarity at the initiation of a natural intracloud lightning flash is not known [*Stanley et al*., 1994; *Krehbiel et al*., 1994; *Shao et al*., 1999]. A delay between positive and negative leaders in the development of a +IC lightning discharge is therefore possible. One of the goals of the present paper is to demonstrate and quantify the effects of such a delay.

4.3. Effect of the delay in initiation of the negative leader on maximum potential differences

[21] Figure 1b shows the potential distributions before the development of the lightning discharge and at the step when the maximum potential difference $\Delta\phi$ between the negative leader tip and the ambient potential is obtained. In this model case, we allow the negative leader to start propagating right after the positive part of the lightning discharge is fully built. Under the conditions discussed above, the potential in the leader channel can be close to the minimum (negative) value of the ambient potential distribution, and thus, the potential difference between its upper end and the ambient distribution at this point can be close to the maximum ambient potential difference that exists in the thunderstorm $\Delta\phi_{amb,max}$ (between the minimum ambient negative potential at ~6 km and the maximum ambient positive potential at ~11 km in Figure 1b).

[22] In Figure 1c, a cross section of the lightning discharge structure is shown at the step when the potential difference between the negative leader tip and the ambient potential is maximum. We see that at that point, the positive leader is extensively developed. *Yoshida et al*. [2010] utilized two interferometers and have estimated the speed of positive lightning leader in a lightning triggering experiment in Florida on the order of 10^6 m/s. If we consider this positive leader speed and if we take into account the delay between the positive and the negative leader initiation 3–6 ms we mentioned in the previous sections, it is clear that the positive leader can be as extensive as shown in this figure before the negative leader starts propagating.

[23] In Figure 1d, the potential difference $\Delta\phi$ between the negative leader tip and the ambient potential at every simulation step is shown. The marked point A shows the simulation step at which the horizontal development of the positive leader begins. Up to that point, the lightning structure is mostly vertical. The point B marks the simulation step corresponding to the initiation of the negative leader. This is also the point at which the potential difference between the negative leader tip and the ambient potential is maximum. In the same figure, the potential difference between the leader tip and the ambient potential at every simulation step is shown for the case of a bidirectional leader without a delay between the initiation of the positive and the negative leaders. We see that the assumed delay of the initiation of the negative leader leads to a potential difference which is ~2.4 times higher than that in the case of no delay. We note that according to *Bazelyan and Raizer* [2000, p. 54], the electric potential of the lightning leader tip with respect to the ambient potential for the case of an unbranched leader channel is approximately $V_0 = E_0 l/2$ where l is the length of the leader channel. In our case, E_0=0.7 kV/cm and the distance between the charges is 5 km, which leads to a potential difference between the leader tip and the ambient potential equal to 175 MV, or similarly $(\Phi_{max} - \Phi_{min})/2$ (see Section 4.1). At point A where the leader channel is vertical, the potential difference is 192 MV, which is indeed close to this value. The horizontal development of the positive leader, with no propagation of the negative leader, further increases this potential difference to 307 MV. Therefore, when the negative leader starts propagating, the potential difference between the leader tip and the ambient potential is ~1.7 times larger than the theoretically estimated for the vertical unbranched channel.

[24] In summary, one can say that the propagation of the positive leader helps bring the minimum ambient potential (Φ_{min}=-110 MV in the present case) close to the upper part of the thundercloud (where $\Phi=\Phi_{max}\simeq$230 MV) through the lightning discharge. The simple propagation of the bidirectional leader without delay would lead to a factor of ~2 lower $\Delta\Phi$.

4.4. Dynamics of Potential Distribution in Thundercloud During Leader Development

[25] In Figure 2, the dynamics of the total potential distribution in the presence of the lightning discharge is shown along the central axis of the simulation domain, for the case of the IC lightning with delay for the initiation of the negative leader with respect to the initiation of the positive leader, at the steps marked in Figure 1d and at the end of the simulation. As the positive leader develops, the potential of the leader channel shifts to values close to the maximum negative value of the ambient potential, increasing the potential difference between the potential at the negative leader tip (which is stalled at the initiation point) and the ambient potential as explained in the previous subsection. As the negative leader starts propagating, it causes a shift of the potential in the leader channel to lower negative values, and at the same time, it modifies the ambient potential to lower positive values, resulting in the reduction of the potential difference between the negative leader tip and the ambient potential. We note that the simulation does not end at the maximum number of steps that is shown in Figure 1d. We present this region for the better visualization of the results. As the negative leader develops inside the positive charge region, the potential difference keeps decreasing. Eventually (after ~10,000 steps for the current

simulation), the potential difference between the negative leader tip and the ambient potential reaches the value of ∼30 MV, and the total potential distribution along the central axis of the simulation domain has the form illustrated in Figure 2.

[26] In the thunderstorm configuration used in this paper, the maximum potential difference is obtained when the negative leader is stalled at the initiation point at the altitude of ∼10.1 km, which is in the range of heights (10.5–14.1 km) of the TGF-related lightning pulses estimated by *Shao et al*. [2010] and the altitude range of the TGF-related lightning leader (10–11 km) estimated by *Lu et al*. [2010].

4.5. Role of the Thundercloud Screening Charges

[27] Although the +IC lightning case presented in this paper does not take into account the screening charges that are induced at the cloud boundaries (see the study by *Riousset et al*. [2010]), we have performed several simulations in the presence of screening charges. We assumed that the thundercloud is a region with low conductivity (similarly to the study by *Riousset et al*. [2010]), and we performed simulations for different altitudes of the upper boundary of the thundercloud. When the thundercloud upper boundary is close to the charge regions and there is a mixing between the screening charges with the cloud charges, there is a reduction of the ambient potential difference between the positive and the negative charge layers because of the reduction of the net positive charge in the cloud. As the distance between the cloud upper boundary and the cloud charge layers increases, the ambient potential difference increases slightly and when the distance becomes equal to ∼4 km, the ambient potential difference converges to the ambient potential difference calculated in the absence of screening charges. In this case, the upper boundary of the thundercloud is located at an altitude of 15 km, which is consistent with observations of the cloud tops of thunderstorms that produce TGFs reported by *Smith et al*. [2010] and *Splitt et al*. [2010]. This suggests that the mixing between the screening charges and the cloud charge layers could obstruct the production of TGFs.

[28] In Table 2, we demonstrate the dependence of the total ambient potential difference on the altitude of the cloud top, when the positive charge layer is at 11 km and the negative charge layer at 6 km. We note that as the mixing between the cloud top screening charges and the positive charge layer increases, then the amount of charge that is required to create electric field, which exceeds the initiation threshold for a lightning discharge (2.16 kV/cm at sea level) by 10%, increases. Since the positive and the negative source charges are equal, there is a corresponding increase of the absolute value of the potential of the negative charge layer. We also note that further decrease of the altitude of the cloud top results in the development of high electric field in the region between the cloud top screening charges and the positive charge layer, which results in the development of an upward jet discharge in the fractal simulations [*Krehbiel et al*., 2008] and not the initiation of an IC lightning. Finally, we note that the presence of the screening charges affects only slightly the ambient potential difference. From Table 2, it is clear that decreasing the distance between the screening charge layer and the main positive layer by ∼2 km leads to a reduction of the ambient potential difference by ∼20 MV. Recalling the significantly greater variation in the ambient potential difference that is caused by the reduction of the distance between the main positive and main negative charge layers (Table 1, see also discussion in Section 4.1), we can conclude that the effect of the presence of the screening charges on the ambient potential difference is not significant.

Table 2. Maximum amplitude of the ambient potential at the center of the negative charge layer (column 2), at the center of the positive charge layer (column 3), maximum ambient potential difference between the two charge layers (column 4), for different values of the altitude of the cloud top (column 1), for the case that the positive charge layer is at 11 km and the negative at 6 km

$h_{cloudtop}$ (km)	Φ_- (MV)	Φ_+ (km)	$\Delta\phi_{amb,max}$ (MV)
15	-156.37	155.08	311.45
14.58	-163.63	147.35	310.98
14	-175.54	134.44	309.98
13.63	-182.74	124.86	307.6
13	-195.28	104.28	299.56
12.65	-201.61	91.28	292.89

5. Conclusions

[29] The main contributions of this work can be summarized as follows:

[30] 1. The potential in the leader channel strongly depends on the ambient potential distribution in the thundercloud. The potential distribution between the two charge layers inside the thundercloud above the conducting ground depends on the total charge in the layers, the distance between these layers, the distance of the lower layer to the ground, and their respective radii. The influence of these parameters is summarized in Table 1. We infer that the weak dependence of the electric potential on the radius of the charge layers can explain the observations of *Splitt et al*. [2010], showing that TGFs are not correlated with large thunderstorm complexes, unlike sprites, but rather occur with thunderstorms ranging in "areal extent by several orders of magnitude" [*Splitt et al*., 2010].

[31] 2. Using a simple model approximation, we have estimated that the maximum total ambient potential difference in a given thundercloud could be achieved for a distance between charge layers equal to the atmospheric scale height $h_s \simeq 8.7$ km. This estimate also leads to a maximum total ambient potential difference possible in a thundercloud of $\Delta\phi_{amb,max}=E_{init}(z=0)h_s/e \simeq 691$ MV.

[32] 3. The development of the positive leader while the negative leader is stalled leads to a shift of the potential of the leader channel to values close to the minimum negative value of the ambient potential. Therefore, the potential difference between the negative leader tip and the ambient potential at this location can be maximized to values close to the ambient potential difference between the minimum negative value and the maximum positive value in the thundercloud. This does not mean that all TGFs are produced in correlation with such a lightning dynamics but rather is informative as to the lightning structures capable of generating very high potential differences. This brings to fore the necessity of further research on the structure and dynamics of the TGF-related lightning discharges.

[33] 4. We found that the mixing between the screening charges that are induced at the cloud boundaries with the cloud charge layers leads to a slight decrease of the ambient potential difference in the thundercloud. In the analyzed realistic configurations, the ambient potential differences are maximized when the cloud boundaries have a distance from the cloud charge layers of at least ∼4 km.

[34] 5. Points 2 and 4 might explain why TGFs are associated with high tropopause heights [*Smith et al*., 2010] and tall thunderclouds [*Splitt et al*., 2010] in addition to the effect of penetration of photons through the atmosphere [*Williams et al*., 2006].

[35] **Acknowledgments.** This research was supported by NSF under grants AGS-0652148 and AGS-1106779 to Pennsylvania State University.

References

Bazelyan, E. M., and Y. P. Raizer (2000), Lightning Physics and Lightning Protection, IoP Publishing Ltd, Bristol, UK and Philadelphia, PA.

Briggs, M. S., et al. (2010), First results on terrestrial gamma ray flashes from the Fermi Gamma-ray Burst Monitor, *J. Geophys. Res.*, *115*, A07323, doi:10.1029/2009JA015242.

Celestin, S., and V. P. Pasko (2011), Energy and fluxes of thermal runaway electrons produced by exponential growth of streamers during the stepping of lightning leaders and in transient luminous events, *J. Geophys. Res.*, *116*(A03315), doi:10.129/2010JA016260.

Celestin, S., W. Xu, and V. P. Pasko (2012), Terrestrial gamma ray flashes with energies up to 100 MeV produced by nonequilibrium acceleration of electrons in lightning, *J. Geophys. Res.*, *117*(A16), A05315, doi:10.1029/2012JA017535.

Dwyer, J. R. (2008), Source mechanisms of terrestrial gamma-ray flashes, *J. Geophys. Res.*, *113*, D10103, doi:10.1029/2007JD009248.

Fishman, G. J., et al. (1994), Discovery of intense gamma-ray flashes of atmospheric origin, *Science*, *264*(5163), 1313.

Gallimberti, I., G. Bacchiega, A. Bondiou-Clergerie, and P. Lalande (2002), Fundamental processes in long air gap discharges, *C. R. Physique*, *3*(10), 1335–1359, doi:10.1016/S1631-0705(02)01414-7.

Gurevich, A. V., G. M. Milikh, and R. A. Roussel-Dupré (1992), Runaway electron mechanism of air breakdown and preconditioning during a thunderstorm, *Phys. Lett. A.*, *165*(5–6), 463–468, doi:10.1016/0375-9601(92)90348-P.

Hedin, A. E. (1991), Extension of the MSIS thermosphere model into the middle and lower atmosphere, *J. Geophys. Res.*, *96*, 1159–1172, doi:10.1029/90JA02125.

Krehbiel, P., X. M. Shao, M. Stanley, G. Gray, C. McCrary, R. Scott, J. Lopez, C. Rhodes, and D. Holden (1994), Interferometer observations of natural and triggered lightning at langmuir laboratory, *Eos Trans. AGU*, *75*(44), Fall Meet. Suppl., Abstract A12C-2.

Krehbiel, P., W. Rison, R. Thomas, T. Marshall, M. Stolzenburg, W. Winn, and S. Hunyady (2004), Thunderstorm charge studies using a simple cylindrical charge model, electric field measurements, and lightning mapping observations, *Eos Trans. AGU*, *85*(47), Fall Meet. Suppl., Abstract AE23A-0843.

Krehbiel, P. R., J. A. Riousset, V. P. Pasko, R. J. Thomas, W. Rison, M. A. Stanley, and H. E. Edens (2008), Upward electrical discharges from thunderstorms, *Nature Geosci.*, *1*(4), 233.

Lalande, P., A. Bondiou-Clergerie, P. Laroche, A. Eybert-Berard, J.-P. Berlandis, B. Bador, A. Bonamy, M. A. Uman, and V. A. Rakov (1998), Leader properties determined with triggered lightning techniques, *J. Geophys. Res.*, *103*, 14,109–14,116, doi:10.1029/97JD02492.

Laroche, P., V. Idone, A. Eybert-Berard, and L. Barret (1991), Observations of bi-directional leader development in a triggered lightning flash, in *1991 International Aerospace and Ground Conference on Lightning and Static Electricity*, pp. 57–1 – 57–10, NASA Conf. P.

Liu, X. S., and P. R. Krehbiel (1985), The initial streamer of intracloud lightning flashes, *J. Geophys. Res.*, *90*(ND4), 6211–6218.

Lu, G., et al. (2010), Lightning mapping observation of a terrestrial gamma-ray flash, *Geophys. Res. Lett.*, *37*(L11806), doi:10.1029/2010GL043494.

Lu, G., S. A. Cummer, J. Li, F. Han, D. M. Smith, and B. W. Grefenstette (2011), Characteristics of broadband lightning emissions associated with terrestrial gamma ray flashes, *J. Geophys. Res.*, *116*(A03316), doi:10.1029/2010JA016141.

Marisaldi, M., et al. (2010), Detection of terrestrial gamma ray flashes up to 40 MeV by the AGILE satellite, *J. Geophys. Res.*, *115*(A14), A00E13, doi:10.1029/2009JA014502.

Marshall, T. C., M. Stolzenburg, C. R. Maggio, L. M. Coleman, P. R. Krehbiel, T. Hamlin, R. J. Thomas, and W. Rison (2005), Observed electric fields associated with lightning initiation, *Geophys. Res. Lett.*, *32*(3), L03813.

Mazur, V. (1989), A physical model of lightning initiation on aircraft in thunderstorms, *J. Geophys. Res.*, *94*(D3), 3326–3340.

Ogawa, T., and M. Brook (1964), Mechanism of intracloud lightning discharge, *J. Geophys. Res.*, *69*(24), 5141.

Press, W. H., B. P. Flannery, S. A. Teukolsky, and W. T. Vetterling (1992), Numerical Recipes in C: The Art of Scientific Computing, second ed., Cambridge Univ. Press, New York, NY.

Proctor, D. E. (1981), VHF radio pictures of cloud flashes, *J. Geophys. Res.*, *86*, 4041–4071.

Raizer, Y. P. (1991), Gas Discharge Physics, Springer-Verlag, New York, NY.

Rakov, V. A., and M. A. Uman (2003), Lightning: Physics and Effects, Cambridge Univ. Press, Cambridge, U.K.; New York.

Riousset, J. A., V. P. Pasko, P. R. Krehbiel, R. J. Thomas, and W. Rison (2007), Three-dimensional fractal modeling of intracloud lightning discharge in a New Mexico thunderstorm and comparison with lightning mapping observations, *J. Geophys. Res.*, *112*, D15203.

Riousset, J. A., V. P. Pasko, P. R. Krehbiel, W. Rison, and M. A. Stanley (2010), Modeling of thundercloud screening charges: Implications for blue and gigantic jets, *J. Geophys. Res.*, *115*, A00E10.

Shao, X. M., and P. R. Krehbiel (1996), The spatial and temporal development of intracloud lightning, *J. Geophys. Res.*, *101*(D21), 26,641–26,668.

Shao, X. M., C. T. Rhodes, and D. N. Holden (1999), RF radiation observations of positive cloud-to-ground flashes, *J. Geophys. Res.*, *104*, 9601–9608, doi:10.1029/1999JD900036.

Shao, X. M., T. Hamlin, and D. M. Smith (2010), A closer examination of terrestrial gamma-ray flash-related lightning processes, *J. Geophys. Res.*, *115*, A00E30, doi:10.1029/2009JA014835.

Smith, D. M., L. I. Lopez, R. P. Lin, and C. P. Barrington-Leigh (2005), Terrestrial gamma-ray flashes observed up to 20 MeV, *Science*, *307*(5712), 1085–1088, doi:10.1126/science.1107466.

Smith, D. M., B. J. Hazelton, B. W. Grefenstette, J. R. Dwyer, R. H. Holzworth, and E. H. Lay (2010), Terrestrial gamma ray flashes correlated to storm phase and tropopause height, *J. Geophys. Res.*, *115*, A00E49, doi:10.1029/2009JA014853.

Splitt, M. E., S. M. Lazarus, D. Barnes, J. R. Dwyer, H. K. Rassoul, D. M. Smith, B. Hazelton, and B. Grefenstette (2010), Thunderstorm characteristics associated with RHESSI identified terrestrial gamma ray flashes, *J. Geophys. Res.*, *115*(D14), A00E38, doi:10.1029/2009JA014622.

Stanley, M., et al. (1994), A 47-stroke triggered lightning discharge, *Eos Trans. AGU*, *75*(44), Fall Meet. Suppl., Abstract A21D-3.

Stanley, M. A., X.-M. Shao, D. M. Smith, L. I. Lopez, M. B. Pongratz, J. D. Harlin, M. Stock, and A. Regan (2006), A link between terrestrial gamma-ray flashes and intracloud lightning discharges, *Geophys. Res. Lett.*, *33*, L06803, doi:10.1029/2005GL025537.

Tavani, M., et al. (2011), Terrestrial Gamma-Ray Flashes as Powerful Particle Accelerators, *Physical Review Letters*, *106*(1), 018501, doi:10.1103/PhysRevLett.106.018501.

Uman, M. A. (1984), Lightning, reprint ed., Dover, Mineola, NY.

Williams, E., et al. (2006), Lightning flashes conducive to the production and escape of gamma radiation to space, *J. Geophys. Res.*, *111*, D16209, doi:10.1029/2005JD006447.

Xu, W., S. Celestin, and V. P. Pasko (2012), Source altitudes of terrestrial gamma-ray flashes produced by lightning leaders, *Geophys. Res. Lett.*, *39*, L08801, doi:10.1029/2012GL051351.

Yoshida, S., et al. (2010), Three-dimensional imaging of upward positive leaders in triggered lightning using VHF broadband digital interferometers, *Geophys. Res. Lett.*, *37*, L05805, doi:10.1029/2009GL042065.